CHAPTER II

THEORY

2.1 Catalysts

A catalyst is a substance that increased the rate of a chemical reaction by reducing the activation energy (E_a) as shown in Figure 2.1 [27]. The highest peak position performing the highest energy refers to the transition state. In typically reaction, the energy required to enter the transition state is high, whereas the energy to transition state decreases in catalytic reaction. In addition, the catalyst may participate in multiple chemical transformations and is not consumed by the reaction.

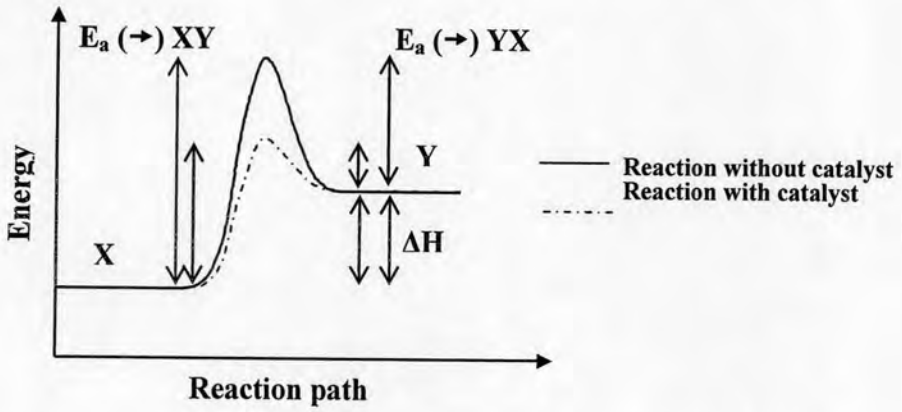

Figure 2.1 The relationship between activation energy (E_a) and enthalpy (ΔH) of the reaction with and without a catalyst.

2.2 Properties of industrial catalysts

The suitable catalysts for industrial processes were considered mainly on the three properties:

2.2.1 Activity is a measure of how fast one or more reactions proceed which can be defined in terms of kinetics. A high activity catalyst will be given high productivity when the less amount of the catalyst was utilized or the reaction was performed in mild operating condition, particularly temperature, which enhances selectivity and stability if the thermodynamic is more favorable. It is appropriate to measure reaction rates in the temperature that will be occurred in the reactor.

2.2.2 Selectivity of a reaction is the fraction of the starting material that is converted to the expected product. High selectivity catalyst produces high yields of a desired product, whereas undesirable competitive and consecutive reactions are suppressed. This means that the texture of the catalyst (in particular pore size and pore volume) should be improved toward reducing limitation by internal diffusion, which in case of consecutive reactions rapidly reduces selectivity.

2.2.3 Stability of a catalyst determines its lifetime in industrial processes. Catalyst stability is influenced by various factors such as decomposition, coking and poisoning. Catalyst deactivation can be followed by measuring activity or selectivity as a function of time. Deactivated catalysts can often be regenerated before they ultimately have to be replaced. The catalyst lifetime is a crucial importance for the economics of process.

Nowadays, the efficient use of raw materials and energy is of major importance, and it is preferable to optimize existing processes than to develop new ones. For various reasons, the target quantities should be given the following order of priority:

Selectivity > Stability > Activity

2.3 Type of the catalysts

Catalysts can be classified into two main types by the boundary of the catalyst and the reactant. Heterogeneous reaction, the catalyst is in a different phase from the reactants, whereas the catalyst in the same phase of reactant is called homogeneous reaction. Thus, the solid catalysts are identified as heterogeneous catalysts, and the liquid catalysts are specified as homogeneous catalysts when assume reactant is liquid. Homogeneous catalysts have a higher degree of dispersion than heterogeneous catalysts only the surface atoms are active [28]. Summary of the advantage and disadvantage of two-type catalyst are presented in Table 2.1.

Table 2.1 Comparison of homogeneous and heterogeneous catalysts

Consideration	Homogeneous catalyst	Heterogeneous catalyst
1. Active centers	All metal atoms	Only surface atoms
2. Concentration	Low	High
3. Selectivity	High	Low
4. Diffusion problems	Practically absent	Present (mass-transfer-controlled reaction)
5. Reaction conditions	Mild (50-200°C)	Severe (often >250°C)
6. Applicability	Limited	Wide
7. Activity loss	Irreversible reaction with product (cluster formation), poisoning	Sintering of the metal crystallites, poisoning
8. Structure/ Stoichiometry	Defined	Undefined
9. Modification possibility	High	Low
10. Thermal stability	Low	High
11. Catalyst separation	Sometimes laborious (chemical decomposition, distillation, extraction)	Fixed-bed: unnecessary Suspension: filtration
12. Catalyst recycling	Possible	Unnecessary (fixed-bed) or easy (suspension)
13. Cost of catalyst losses	High	Low

The major disadvantage of homogeneous catalyst is the difficulty of separating the catalyst from the product. Heterogeneous catalysts are either automatically removed in the process (e.g. vapour-phase reaction in fixed bed reactor) or separated by simple methods such as filtration or centrifugation. However, in more complicated processes, for the example distillation, liquid-liquid extraction and ion exchange are necessarily used homogeneous catalysts.

2.4 Porous molecular sieves

Molecular sieves are porous materials that exhibit selective adsorption properties which can be classified on the IUPAC definitions into three main types depending on their pore sizes that are microporous materials, mesoporous materials, and macroporous materials. Properties and examples of these materials are shown in Table 2.2.

Table 2.2 IUPAC classification of porous materials

Type of porous molecular sieve	Pore size (Å)	Examples
Microporous materials	< 20	Zeolites, Activated carbon
Mesoporous materials	20 – 500	M41s, SBA-15, Pillared clays
Macroporous materials	> 500	Glasses

Zeolites are one of the microporous molecular sieves with crystalline aluminosilicates of alkali and alkaline earth metals. They are both occurred in nature and archived from the syntheses. The unique properties of zeolites i.e. high surface area, high sorption, high acidity and active site for ion exchange have been exploited for their catalytic applications such as petrochemical industry, oil refining (as cracking catalysts and as adsorbents) and synthesis of chemicals.

2.4.1 Basic units of zeolites

A zeolite has a three dimensional network structure of tetrahedral primary building units (PBU) which make of four oxygen anions with either silicon [SiO_4] or aluminum [AlO_4]$^-$ cations in the center as shown in Figure 2.2(a). Then, secondary building units (SBU) consist of selected geometric groupings of those tetrahedra by oxygen bridges as shown in Figure 2.2(b).

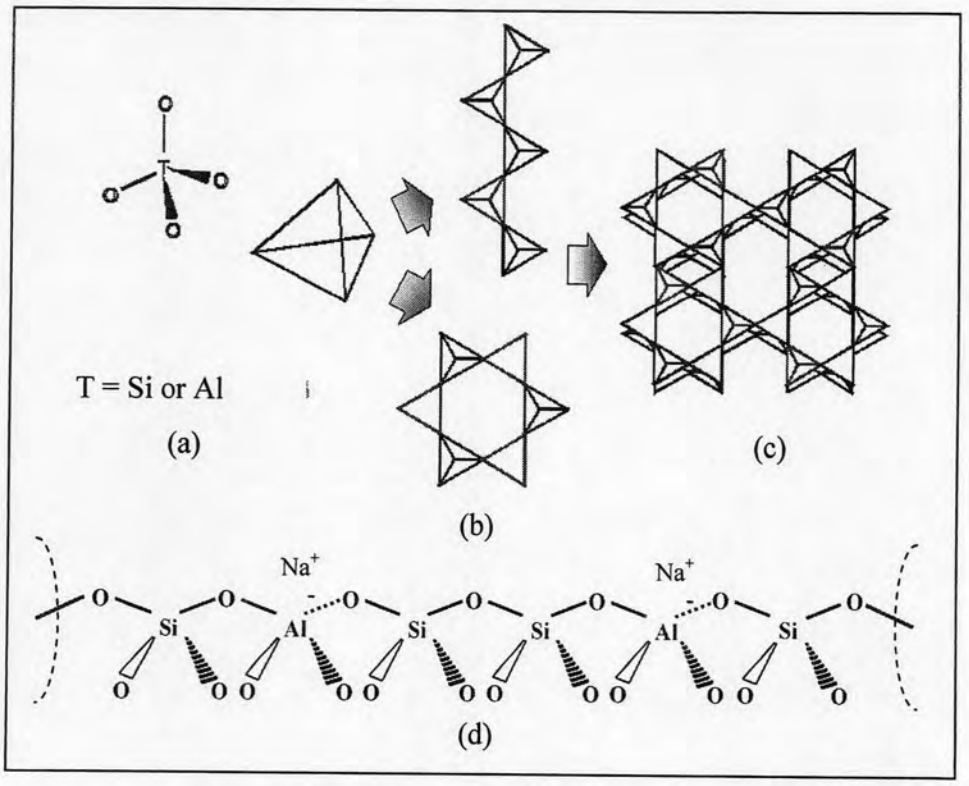

Figure 2.2 A primary building unit (a), secondary building unit (b), framework of a zeolite (c), and metal ions balancing the framework charges of a zeolite (d).

The tetrahedra are mutually connected by sharing oxygen atoms as shown in Figure 2.2(c) which produce the framework of zeolites. The negative charges of the lattices are neutralized by the positive charges of the metal cations. In the normal form of zeolites, these are usually cations of univalent and bivalent metals or their combination (Figure 2.2(d)).

2.4.2 Channel structure in zeolites

The nature of interconnecting channel in zeolites is important in determining the physical and chemical properties. Three types of channel system are illustrated in Figure 2.3.

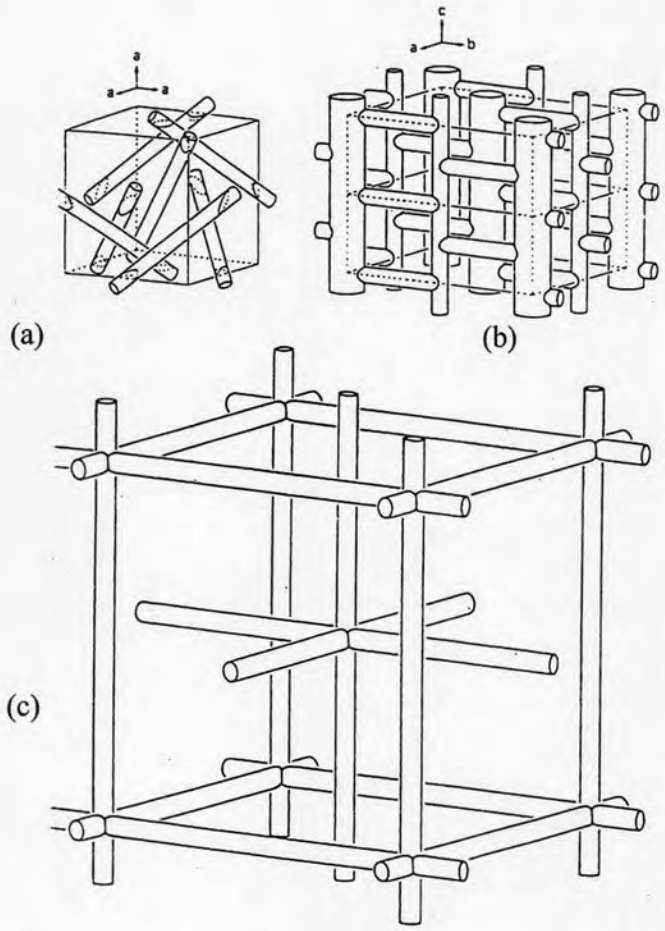

Figure 2.3 Three types of channel in zeolites (a) one-dimension system of analcime structure, (b) two-dimension system of mordenite structure, and (c) three-dimension system of paulingite structure [29].

1. One-dimension system: The channels do not intersect together that is found in analcime as shown in Figure 2.3 (a).

2. Two-dimension system: The main parallel channels are crossed by perpendicular channels but the channels between the sheets are not linked such as mordenite in Figure 2.3 (b).

3. Three-dimension system: This system can be divided into two types. The former, the channels are equidimensional, the diameters of all channels are equal, regardless of direction. The latter consists of three-dimension intersecting channels, but the channels are not equidimensional. The diameters depend upon the crystallographic direction.

2.4.3 Properties of zeolites

2.4.3.1 Shape and size selectivity

The ability of zeolites to preferentially select molecules can be used in many useful applications. If a reactant is sterically unable to enter the zeolite pore, where the reaction takes place, then the product resulting from that reactant is also restricted (Figure 2.4). In the second case, if a product forms inside the zeolitic cavity but is unable to leave, it is restricted again (Figure 2.5).

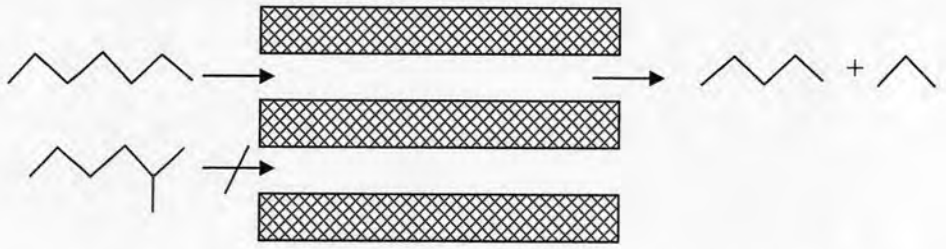

Figure 2.4 Schematic diagram of reactant shape selectivity: rejection of branched chain of hydrocarbons.

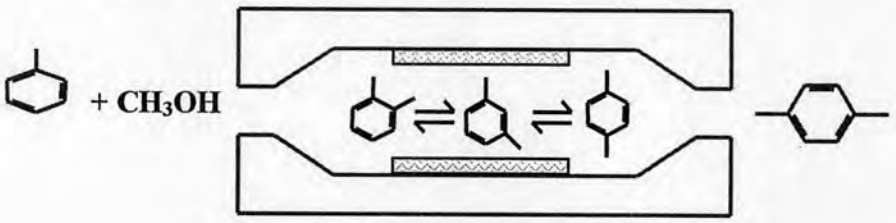

Figure 2.5 Schematic diagram of product shape selectivity: p-xylene diffuses preferentially out of the zeolite channels.

2.4.3.2 Acidity of zeolites

Besides the shape and size selective catalysis, the generation of acidic sites in the zeolite pores leads to a highly efficiency in solid-acidic catalysis. The isomorphous replacement of silicon atom with aluminum atom in a tetrahedral site gives rise to a charge imbalance because aluminum atom has lower coordination ability than silicon atom and must be neutralized. This is achieved in two ways in natural zeolites:

- The length of Al-O bond becomes slightly longer.
- A coordination site is made avail for cation to counter the excess negative charge.

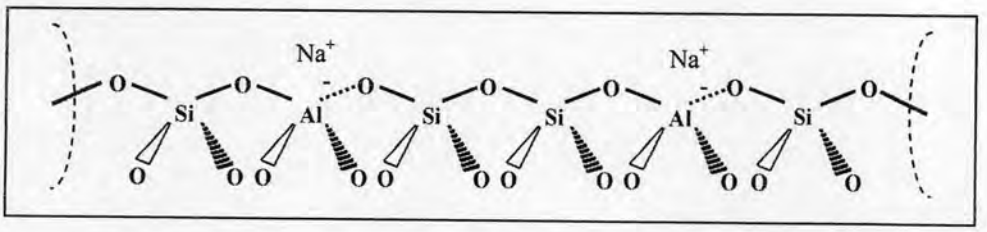

Figure 2.6 Sodium balanced zeolite framework [30].

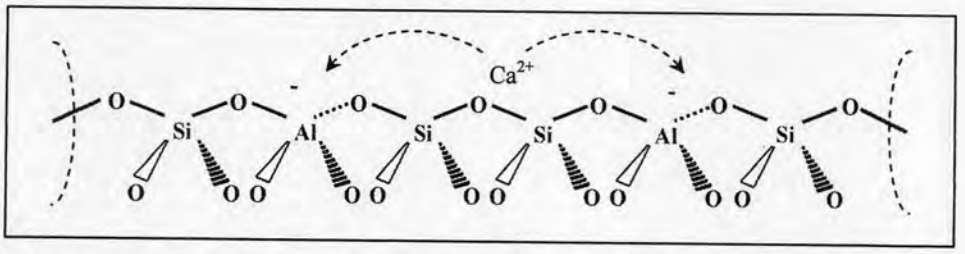

Figure 2.7 Calcium balanced zeolite framework [30].

In natural zeolites, the excess negative charge is balanced by various cations are present in the neighbouring environment e.g. K^+, Na^+, $Mg^{2+}$and Ca^{2+} as exhibited in Figure 2.6 and Figure 2.7. The type of counter ion used to balance the charge plays an important part in the use of the zeolite. For uncomplicated understanding, the cation is replaced with a proton by hydrothermal treatment to form a hydroxyl group at the sharing oxygen atom. The acid site formed behaves as a classic Brønsted, proton donating acidic site as shown in Figure 2.8.

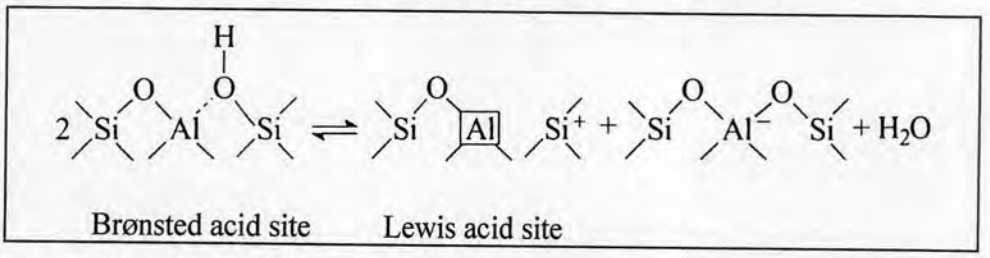

Figure 2.8 Brønsted and Lewis acid sites in zeolites [28].

The highly acidic sites combined with the high selectivity arising from shape selectivity and large internal surface area makes the zeolite as an ideal industrial catalyst. The significance of this acidic proton can be shown easily by comparisons of the experiments in H^+-exchanged zeolites and their equivalent cation from zeolite. For example, the methanol-to-gasoline (MTG) process is highly depended on the presence of the Brønsted proton. If the H-ZSM-5 catalyst is replaced by the purely siliceous analogue of ZSM-5, it has no Brønsted protons, the reaction does not take place at all.

Therefore, the modification of zeolite structure can be increased their activity, which are very economically important step for industry.

2.5 Mesoporous materials

Mesoporous materials are a type of molecular sieves, such as silicas or transitional aluminas or modified layered materials such as pillared clays. Mesoporous silica has uniform pore sizes from 20 to 500 Å and has found great utility as catalysts and sorption media because of the regular arrays of uniform channels. Larger surface area is desired for enhancing of the efficient in the reactions.

2.5.1 Classification of mesoporous materials

Mesoporous materials can be classified by different synthetic methods into three categories as described in Table 2.3.

Table 2.3 Classification of mesoporous materials by synthetic procedures

Assembly	Template	Media	Material
(i) Electrostatic	Quaternary ammonium salt	Base or acid	MCM-41
(ii) H-bonding	Primary amine	Neutral	HMS
(iii) H-bonding	Amphiphilic triblock copolymer	Acid (pH<2)	SBA-15

2.5.2 Synthesis strategies of mesoporous materials

Crystalline molecular sieves are generally obtained by hydrothermal crystallization. The gel composition usually contains cation species (e.g. Si^{4+} for silicate materials, Al^{3+} for aluminate materials) to form the framework, anionic species (e.g. OH^- and Br^-), organic template and solvent (generally water). Typically, the nature of template can be considered into two parts that are hydrophobic tail on the alkyl chain side and hydrophilic head on the other side. The examples of template used are primary, secondary, tertiary, and quaternary amines, alcohols, crown or linear ethers, and as well as polymer. An understanding of how organic molecules interact with each other and with the inorganic frameworks would increase the ability to design rational routes to molecular sieve materials. The organic templates are frequently occurred in the pores of the synthesized material, contributing to the stability of mineral backbone.

2.5.2.1 The behavior of surfactant molecules in an aqueous solution

In a simple binary system of water-surfactant, surfactant molecules can aggregate to form micelles in various types at a particular concentration. The shapes of micelle depend on the concentrations as shown in Figure 2.9.

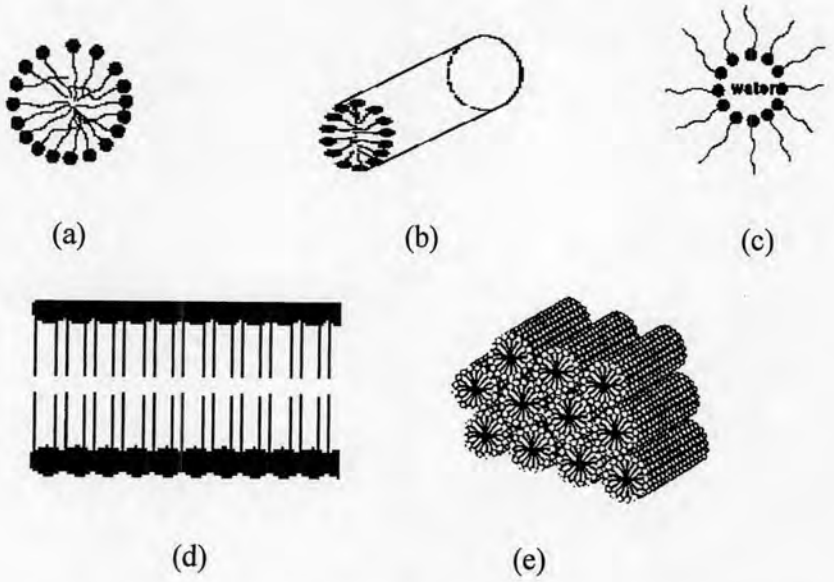

Figure 2.9 Phase sequence of the surfactant-water binary system (a) spherical micelle, (b) rod-shaped micelle, (c) reverse micelle, (d) lamellar phase, and (e) hexagonal phase.

At low concentration, they energetically exist as isolated molecules. With increasing concentration, surfactant aggregate together to form isotropic spherical and rod shaped micelles by directing the hydrophobic tails inside and turning the hydrophilic heads outside in order to decrease the system entropy. The initial concentration threshold at which those molecules aggregate to form isotropic micelle is called critical micelle concentration (CMC). The CMC determines thermodynamic stability of the micelles. When the concentration is continuously increased, the micellar shape changes from sphere or rod shapes to hexagonal, lamellar, and inverse micelles. The particular phase present in a surfactant aqueous solution depends not only on the concentrations but also on the natural of surfactant molecules such as its length of the hydrophobic carbon chain, hydrophilic head group,

and counter ion. Besides the ionic strength, pH value, and temperature including other additives are the factors determining the shape of micelles.

2.5.2.2 Interaction between inorganic species and surfactant micelles

The major components of framework structure, mainly silicate, present in aqueous solution as inorganic species. To acquire the desired structure, firstly, the template forms the proper shape, and then the inorganic soluble species interact with the surfactant as shown in Table 2.4. The hybrid solids formed are strongly depended on the interaction between the surfactant and the inorganic precursors.

Table 2.4 Example routes for interactions between the surfactant and the inorganic soluble species

Surfactant type	Inorganic type	Interaction type	Example materials
Cationic (S^+)	I^-	S^+I^-	MCM-41, MCM-48
	I^+X^-	$S^+X^-I^+$	SBA-1, SBA-2, Zinc phosphate
	I^0F^-	$S^+F^-I^0$	Silica
Anionic (S^-)	I^+	S^-I^+	Al, Mg, Mn, Ga
	I^-M^+	$S^-M^+I^-$	Alumina, Zinc oxide
Neutral S^0 or N^0	I^0	S^0I^0 or N^0I^0	HMS, MSU-X, Aluminum oxide
	I^+X^-	$S^0X^-I^+$	SBA-15

where S^x or N^x : surfactant with charge of X,

I^x : inorganic species with charge of X,

X^- : halogenide anions,

F^- : fluoride anion,

M^{n+} : metal with charge of X.

In case of ionic surfactant (S^+ and S^-), the hydrophilic head mainly binds with inorganic species through electrostatic interactions. There are two possible formation routes. Firstly, direct pathway: surfactant and inorganic species of

which charges are opposite interact together directly (S^+I^- and S^-I^+). Another is the indirect pathway, occurring when the charges of surfactant and inorganic species are the same, so the counter ions in solution get involved as charge compensating species for example the $S^+X^-I^+$ path takes place under acidic conditions, in the present of halogenide anions (X^- = Cl^- or Br^-) and the S^-M^+ I^- route is the characteristic of the basic media, in the existence of alkaline cation (M^+ = Na^+ or K^+). Figure 2.10 shows the possible hybrid inorganic-organic interfaces.

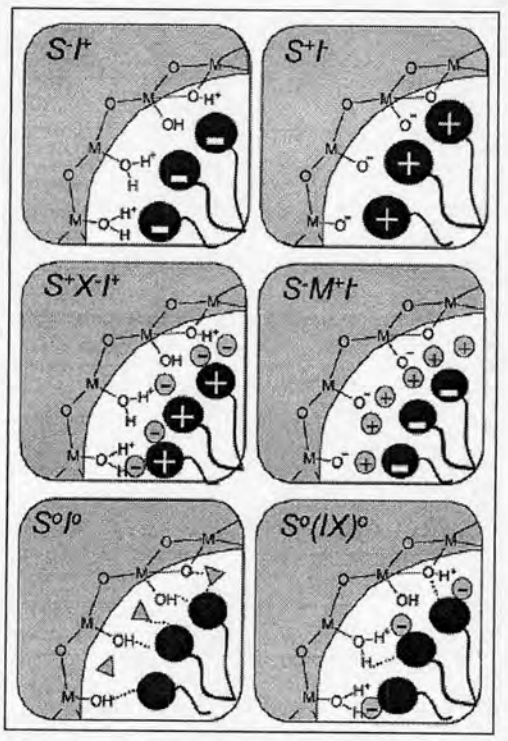

Figure 2.10 Schematic representation of the different types of silica-surfactant interfaces (dashed line corresponded to H-bonding interactions) [31].

Using non-ionic surfactant (S^0 or N^0), the main interaction between template and inorganic species is hydrogen bonding or dipolar, which is called neutral path i.e. S^0I^0 and $S^0F^-I^+$. Nowadays, non-ionic surfactants give important commercial advantages in comparison to ionic surfactants because they are easily removable, nontoxic, biodegradable and relatively inexpensive.

2.5.2.3 Formation mechanism of mesoporous materials

Mechanism of mesoporous formation can be classified on the basis of synthetic route into three types exhibited in Figure 2.11.

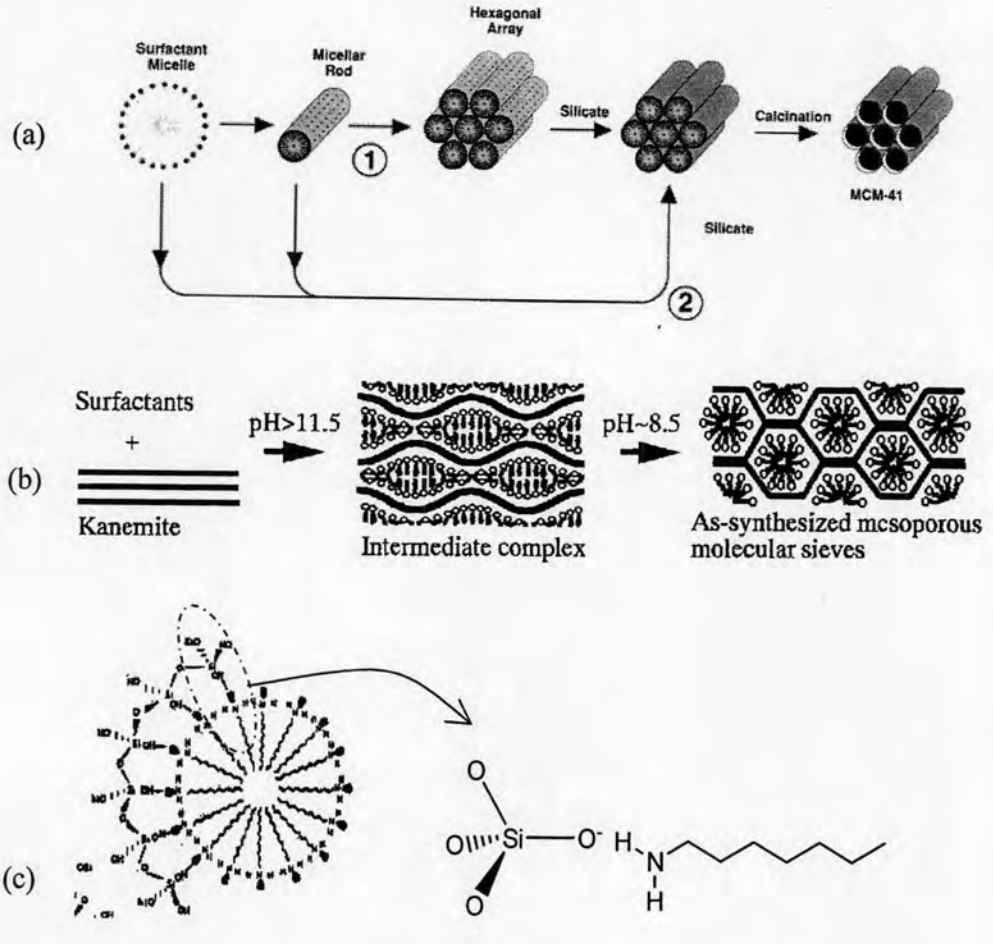

Figure 2.11 Mechanism of mesoporous formation (a) Liquid crystal templating mechanism of MCM-41 formation, (b) Folding sheet formation of FSM-16 formation and (c) H-bonding interaction in HMS formation [32-33].

(a) *Liquid crystal templating mechanism*: i.e. MCM-41. From Figure 2.10(a) there are two main pathways; firstly, liquid crystal phase was intact before silicate species were added or another pathway is the addition of the silicate results in the ordering of the subsequent silicate-encased surfactant micelles.

(b) *Folding sheet formation*: i.e. FSM-16. The intercalation of ammonium surfactant into hydrate sodium silicate, which composes of single layered silica sheets called "kanemite" (ideal composition $NaHSi_2O_5 \cdot 3H_2O$), produces the lamellar-to-hexagonal phase in FSM-16 formation. After the surfactants were ion exchanged into layered structure, the silicate sheets were thought to fold around the surfactants and condense into a hexagonal structure.

(c) *Hydrogen-bonding interaction*: i.e. HMS, SBA-15. The neutral template produces mesoporous materials with thicker walls and higher thermal stability as compared to the LCT-derived silicates.

Although some of mesoporous as described above have the same hexagonal structure, they are different in the properties as shown in Table 2.5. Since the thermal and hydrothermal stability of material are based on the wall thickness, therefore, from Table 2.5 SBA-15 possesses and exhibits significantly higher thermal and hydrothermal stability than other materials. Furthermore, its pore sizes can be expanding up to 300 Å which allow the bulky molecules to diffuse into the pores.

Table 2.5 Properties of some hexagonal mesoporous materials

Mesoporous Material	Pore size (Å)	Wall thickness (nm)	BET specific surface area (m^2/g)
MCM-41	15-100	1	>1000
HMS	29-41	1-2	640-1000
FSM-16	50-300	no report	680-1000
SBA-15	46-300	3-6	630-1000

2.5.3 Synthesis strategy of mesoporous material using block-copolymer as structure directing agent

In the synthesis of MCM-41 and FSM-16, alkyltrimethyl ammonium ion (C_nTA^+, $8<n<18$) as the cationic surfactant and tertiary amine ($C_nH_{2n+1}N^+(CH_3)_3$) as anionic surfactant are used as template, respectively. These syntheses were done in extreme alkaline ($pH \geq 10$) condition and the obtained materials having pore sizes in the range of 15 to 100 Å only. However, by this mean, two limitations occurred:

(1) The obtained materials perform lower stability due to the thinner wall thickness of materials (8-13 Å).

(2) The pore size is difficult to expand because the ionic surfactants give a limited pore size. The way to expand the pore size is only in employing swelling agents such as 1,3,5-trimethyl benzene, involving complicate synthesis.

Thus, the block copolymer has been used to solve these problems. Generally, amphiphilic block copolymer has been used in the field of surfactants, detergent manufacturing, emulsifying, coating, etc. The properties of block copolymer can be continuously tuned by adjusting solvent composition, molecular weight, or type of polymers. Figure 2.12 shows typical block copolymers used as templates.

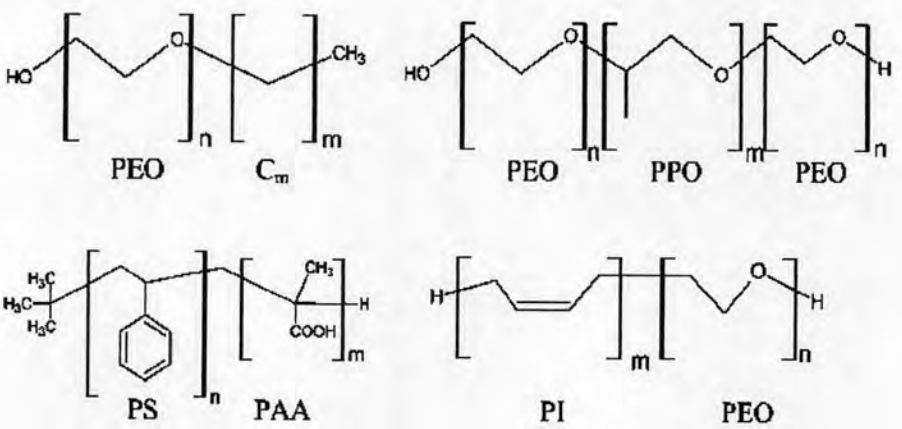

Figure 2.12 Block copolymers used in mesostructured generation [34].

Some advantages of using these block copolymers are:

(1) *The thicker wall thickness* (about 15-40 Å) enhances hydrothermal and thermal stability of materials.

(2) *Pore diameter can be tuned easier* by varying type or concentration of polymer.

(3) *Ease to remove from mineral framework* by thermal treatment or solvent extraction. Due to the hydrogen bonding interaction between template and inorganic framework, therefore, it should be easier to dissociate as compared to ionic templates (electrostatic interaction).

Interaction between block copolymer template and inorganic species, called hybrid interphase (HI), is particularly important, especially in PEO-PPO based one. Different possible interactions taking place at the HI are shown in Figure 2.13. Most of the fine HI characterizations have been performed on PEO-based (di or triblock) templates. Melosh *et al.* [34] determined that the organization arose for polymer weight fractions higher than 40% in F127-templated silica monoliths. For lower polymericsilica ratios, non-ordered gels were formed. This lack of order was due to a relatively strong interaction (probably of H-bonding type) of the (Si-O-Si) polymers forming the inorganic skeleton with both PEO and PPO blocks.

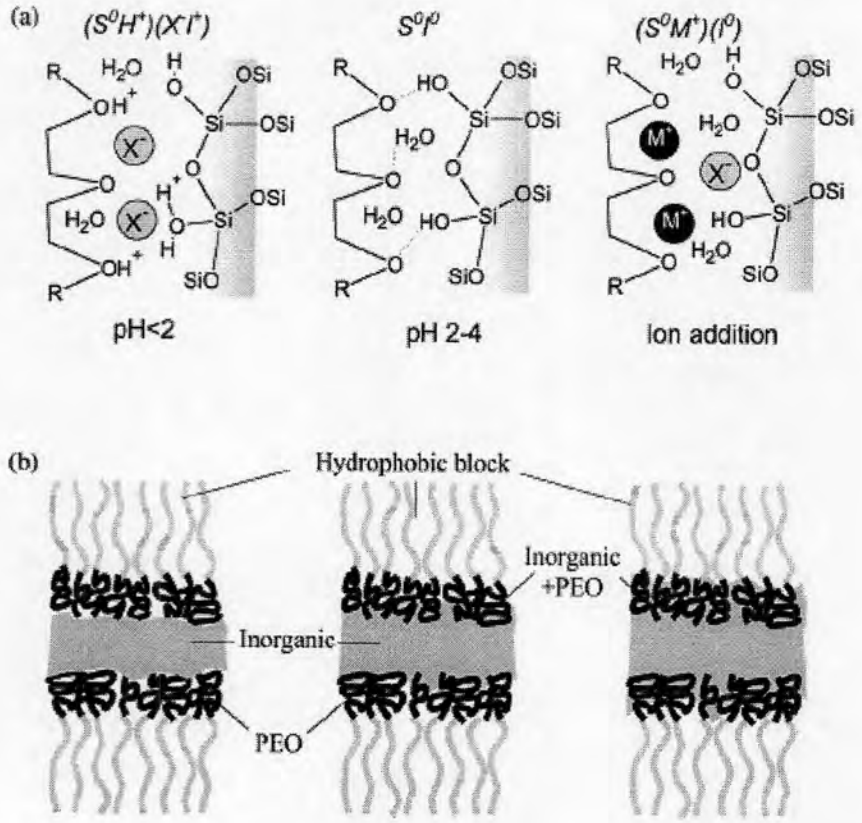

Figure 2.13 (a) Schematic view of the $(S^0H^+)(X^-I^+)$, S^0I^0, and $(S^0M^+)(X^-I^0)$ hybrid interphases (HIs), (b) Three possible structures of a HI composed by a nonionic polymer and an inorganic framework [31].

2.6 SBA-15

2.6.1 Structure and properties of SBA-15

SBA-15 mesoporous material has been synthesized under acidic condition using triblock copolymer as a structure directing agent. This mesoporous material has shown higher hydrothermal stability as compared to MCM-41 due to its higher wall thickness (3.1-6.4 nm). They also pose uniform and hexagonal-structured channel similar to MCM-41 as shown in Figure 2.14 with larger pore size which make them more desirable to deal with bulky molecule. Some properties of MCM-41 and SBA-15, two well-known mesoporous materials, are compared as described in Table 2.6. According to the properties listed in Table 2.6, SBA-15 shows a better performance than MCM-41 in almost of properties.

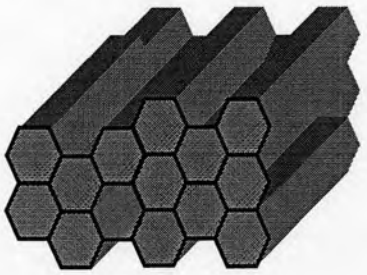

Figure 2.14 Hexagonal mesoporous structure.

Table 2.6 Comparison of two well-known mesoporous materials, MCM-41 and SBA-15 in their characteristic properties [21, 23]

Properties	MCM-41	SBA-15
Pore size (Å)	20-100	46-300
Pore volume (mL/g)	>0.7	0.8-1.23
Surface area (m^2/g)	>1000	690-1040
Wall thickness (Å)	10-15	31-64

2.6.2 Synthesis of SBA-15 and formation mechanism

For SBA-15 material, the aging time and the aging temperature are particularly important factors for the synthesis. Some research found that mesoporous SBA-15 prepared from calcination of an 'as-prepared' hybrid precursor contained a significant fraction of microporosity. Further, aging of the precursor in the mother liquors leads to an improvement on the pore size distribution (Figure 2.15), in agreement with the first work by Stucky *et al.* [23].

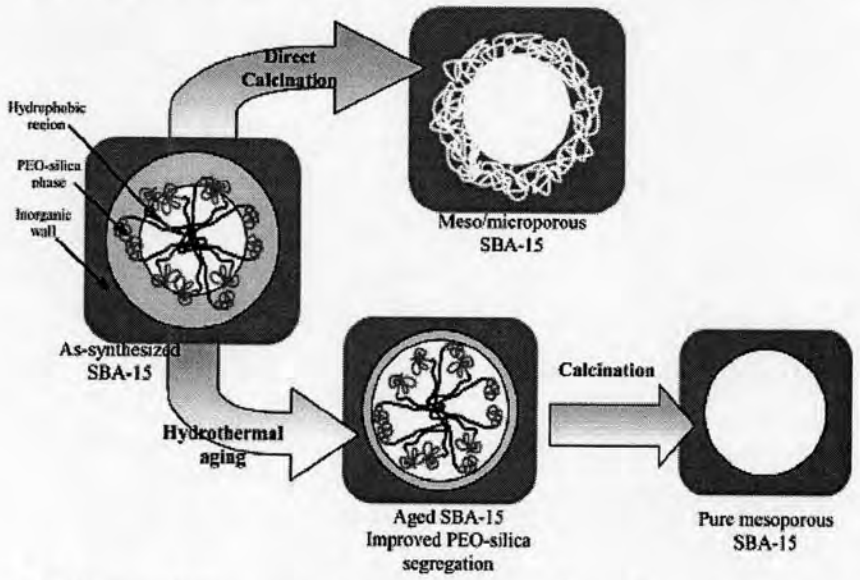

Figure 2.15 Pore evolution upon thermal treatment, depending on pre-treatment and aging [31].

Aging of an as-prepared precipitate at 80–100°C seems to activate the segregation of the PEO blocks and the inorganic framework by promoting condensation of the latter. High temperatures also change the polymer behavior. It is known that PEO blocks become less hydrophilic at the temperature is higher than 60°C, while PPO blocks expel water at the temperature is higher than 40°C [31]. For a mechanism, firstly alkoxysilane species (TMOS or TEOS) are hydrolyzed as:

$$Si(OEt)_4 + nH_3O^+ \xrightarrow[pH<2]{\text{hydrolysis}} Si(OEt)_{4-n}(H_2O^+)_n + n\,EtOH$$

which is followed by partial oligomerization at the silica. Furthermore, at this condition, the PEO parts of surfactant associate with hydronium ions as followed:

$$-PEO_m- + yHX \xrightarrow{H_2O} -PEO_{m-y}[(EO)\cdot 3H_2O^+]_y \text{---} X_y^-$$

Next, coordination sphere expansion around the silicon atom by anion coordination of the form $X^-SiO_2^+$ may play an important role. The hydrophilic PEO blocks are expected to interact with the protonated silica and thus be closely associated with the inorganic wall. During the hydrolysis and condensation of the silica species, intermediate mesophase is sometimes observed and further condensation of silica species and organization of the surfactant and inorganic species result in the formation of the lowest energy silica-surfactant mesophase structure allowed by solidifying network.

2.6.3 Incorporation of aluminum into SBA-15

Among the metal-substituted mesoporous materials, aluminum-incorporated mesoporous materials have the great potential in moderating acid-catalyzed reactions for large molecules. However, it is very difficult to introduce the metal ions directly into SBA-15 due to the easy dissociation of metal-O-Si bonds under strong acidic conditions.

2.6.3.1 Direct synthesis method

To date, only a few studies on the direct synthesis of Al-SBA-15 have been reported [35-37]. The comparison of direct and post syntheses of Al-SBA-15 is described in Table 2.7.

Table 2.7 Comparison of direct synthesis and post synthesis methods of Al-SBA-15 [24, 35-38]

	Direct synthesis method	**Post synthesis method**
Synthesis condition	Require complicated procedure	Simple method
Aluminum form in materials	Most of samples have both tetrahedral and octahedral aluminum	Most of samples have only tetrahedral aluminum
Catalyst activity	Lower activity due to extra-framework aluminum	Higher activity due to aluminum in framework

The direct synthesis of Al-SBA-15 is difficult and often not stoichiometric. From this viewpoint, therefore, the development of a simple post

synthesis method for the alumination of the mesoporous silicas that are synthesized under strongly acidic conditions becomes an appealing alternate choice.

2.6.3.2 Post synthesis of Al-SBA-15

Nowadays, several post synthesis method where aluminum was grafted onto the mesoporous wall with various aluminum sources such as $Al(CH_3)_3$, $AlCl_3$ have been developed without the mesoporous structure seriously destroyed [39]. In the case of zeolites, the introductions of Al into their framework will lead to the formation of bridging hydroxyl groups (Brønsted acid sites). However, whether the similar situation occurs in mesoporous materials still keeps argument. Some researchers assigned the hydroxyl vibration at about 3606 cm^{-1} in IR spectrum to the acidic bridging hydroxyl groups, while others disagreed with the assignment. For example, Trombetta *et al.* argued that the Brønsted acid sites in mesoporous materials or aluminosilicates resulted from terminal silanol groups in the vicinity of aluminum atoms [39]. After the adsorption of a basic probe, such as pivalonitrile, the terminal silanol groups were induced to form the bridging hydroxyl groups (SiOHAl, shown in Figure 2.16).

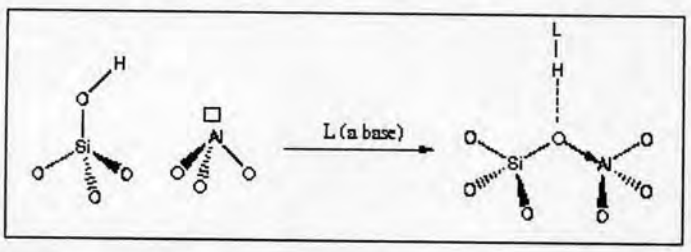

Figure 2.16 Alumination of mesoporous material using basic probe (L) inducing to form the bridging hydroxyl group [36].

2.7 Characterization of mesoporous hexagonal structure

Reliable characterization of the porous hexagonal structure requires the use of six independent techniques:

(a) Powder X-ray diffraction (XRD)

(b) Scanning electron microscope (SEM)

(c) Nitrogen adsorption-desorption technique

(d) Inductively coupled plasma-atomic emission spectroscopy (ICP-AES)

(e) Solid state ^{27}Al-nuclear magnetic resonance (^{27}Al-MAS-NMR)

(f) Temperature-programmed desorption (TPD) of ammonia

2.7.1 Powder x-ray diffraction (XRD) [40]

X-ray powder diffraction (XRD) is a reliable technique that can be used to identify hexagonal-mesoporous structure which perform five well-resolved peaks corresponding to lattice planes of Miller indices (100), (110), (200), (210), and (300). These XRD peaks appear at low angle (2θ angle between 2 and 5 degree) due to the materials are not crystalline at atomic level, thus, the diffraction at higher angles are not observed.

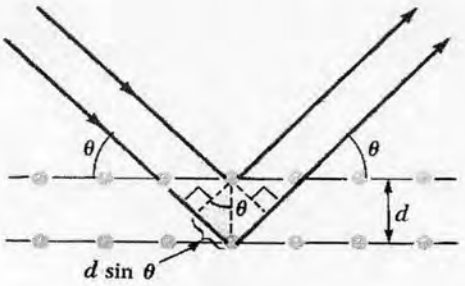

Figure 2.17 Diffraction of X-ray by regular planes of atoms.

Figure 2.17 shows a monochromatic beam of X-ray incident on the surface of crystal at an angle, θ. The scattered intensity can be measured as a function of scattering angle 2θ. The resulting XRD pattern efficiently determines the different phases present in the sample structure. Using this method, Bragg's law is able to determine the interplanar spacing of the samples from diffraction peak according to Bragg's angle.

$$n\lambda = 2d\sin\theta$$

where the integer n is the order of the diffracted beam, λ is the wavelength, d is the interplanar distance of the crystal (the d-spacings) and θ is the angle of between the incident beam and these planes.

2.7.2 Scanning electron microscope (SEM) [41]

The scanning electron microscope (SEM) has unique capabilities for analyzing surfaces and morphology of materials. It is analogous to the optical microscope, although different radiation sources serve to produce the required illumination. Whereas the optical microscope forms an image from light reflected from a sample surface, the SEM uses electrons for image formation. The different

wavelengths of these radiation sources result in different resolution levels: electrons have much shorter wavelength than light photons, and shorter wavelengths are capable of generating the higher resolution information. Enhanced resolution in turn permits higher magnification without loss of detail. The maximum magnification of the light microscope is about 2,000 times; beyond this level is "empty magnification", or the point where increased magnification does not provide additional information. This upper magnification limit is a function of the wavelength of visible light, 2000 Å, which equals the theoretical maximum resolution of conventional light microscope. In comparison, the wavelength of electron is less than 0.5 Å. Theoretically, the maximum magnification of electron beam instrument is beyond 800,000 times because of instrumental parameters. Practical magnification and resolution limits are about 75,000 times and 40 Å, respectively, in a conventional SEM. The SEM consists basically of four systems:

1. The *illuminating/imaging system* produces the electron beam and shoots it onto the sample.
2. The *information system* includes the data released by the sample during electron bombardment and detectors which discriminate among these analyzed information signals.
3. The *display system* consists of one or two cathode-ray tubes for observing and photographing the surface of interest.
4. The *vacuum system* removes gases from the microscope column which increase the mean free path of electron, hence the better image quality.

2.7.3 Nitrogen adsorption-desorption technique [42-43]

The N_2 adsorption-desorption technique is used to classify the porous material and its physical properties such as surface area, pore volume, pore diameter and pore-size distribution of solid catalysts. Characteristic of porous material is described by an adsorption isotherm, while total specific surface area is correlated to the amount of adsorbed gas by the material at a fixed temperature as a function of pressure. Pore volume, pore diameter and pore size are frequently derived from gas sorption data. The IUPAC classification of adsorption isotherms is illustrated in Figure 2.18.

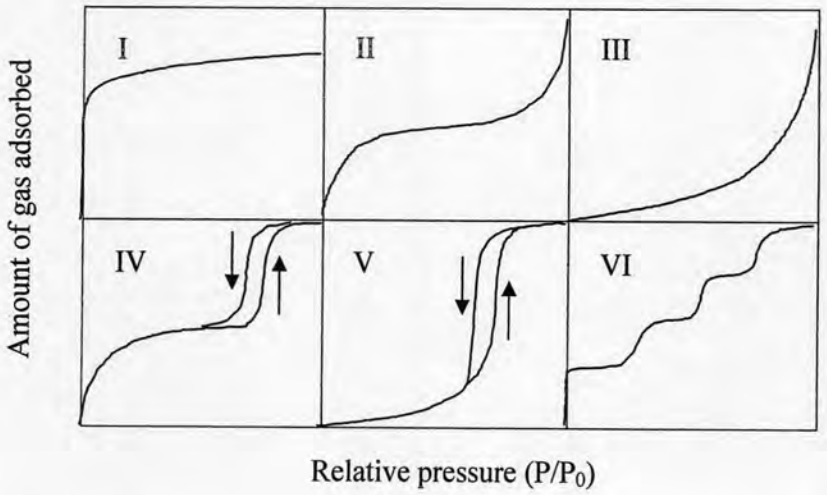

Figure 2.18 The IUPAC classification of adsorption isotherms.

Adsorption isotherms are described as shown in Table 2.10 based on the strength of the interaction between the sample surface and the adsorbate. Pore size distribution is measured by the use of nitrogen adsorption/desorption isotherm at liquid nitrogen temperature and the relative pressures (P/P_o) ranging from 0.05-0.1. The large uptake of nitrogen at low P/P_o indicates filling of the micropores (<20 Å) in the adsorbent. The linear portion of the curve represents multilayer adsorption of nitrogen on the surface of the sample, and the concave upward portion of the curve represents filling of mesoporous and macropores. The multipoint Brunauer, Emmett and Teller (BET) method is commonly used to measure total surface area.

$$\frac{1}{W[(P_o/P)-1]} = \frac{1}{W_m C} + \frac{C-1}{W_m C}(P/P_o)$$

where W is the weight of nitrogen adsorbed at a given P/P_o, and W_m is the weight of gas to give monolayer coverage, and C is a constant that is related to the heat of adsorption. A slope and intercept are used to determine the quantity of nitrogen adsorbed in the monolayer and calculated the surface area. For a single point method, the intercept is taken as zero or a small positive value, and the slope from the BET plot is used to calculate the surface area. The surface area reported depend upon the method used, as well as the partial pressures at which the data are collected.

Table 2.8 Features of adsorption isotherms

Type	Interaction between sample surface and gas adsorbate	Porosity	Example of sample-adsorbate
I	Relatively strong	Micropores	Activated carbon-N_2
II	Relatively strong	Nonporous	Oxide-N_2
III	Weak	Nonporous	Carbon-water vapor
IV	Relatively strong	Mesopore	Silica-N_2
V	Weak	Micropores	
		Mesopore	Activated carbon-water vapor
VI	Relatively strong sample surface has an even distribution of energy	Nonporous	Graphite-Kr

2.7.4 Inductively coupled plasma – atomic emission spectroscopy (ICP-AES) [44]

It is essential to determine elemental composition to be assured that the composition of active elements in catalyst is closed to what expected. It is also often used in explanation of the life time of catalyst by using the elemental composition of catalyst. To do these, chemical methods of analysis such as ICP-AES, XRF are still in use.

2.7.5 Solid state ^{27}Al-nuclear magnetic resonance (^{27}Al-MAS-NMR) [29, 45]

NMR has established itself as a major and unique analytical tool in the characterization on the structural features of solid materials including zeolites and other aluminosilicates since 1980. Table 2.9 shows the relevant nuclei, the directly relevant nuclei in zeolite studies are ^{29}Si and ^{27}Al-NMR which provide framework or structural information about zeolites or mesoporous molecular sieves.

An advantage in examining ^{27}Al-NMR spectra is that ^{27}Al has a 100 percent natural abundance with $I = 5/2$ and ranges in chemical shift about 450 ppm. Quadrupole coupling must be separated from chemical shift effect to render useful chemical information from ^{27}Al-NMR spectrum. For the low Si/Al molar ratios where

the Si resonances are very weak in the ^{29}Si-NMR spectra, incorporation of Al in the framework can readily be demonstrated *via* ^{27}Al-NMR. The ^{27}Al-NMR has been used mainly for the detection of aluminum in extra-framework, since the ^{27}Al-NMR chemical shifts depend primarily on the coordination of aluminum with respect to oxygen. For octahedral coordination, chemical shifts of 0 to 22 ppm from $Al(H_2O)_6^{3+}$ are observed. Tetrahedral Al appears at 55 to 80 ppm. Both the solid and solution spectra show similar ranges. The position of the signal in ^{27}Al-NMR spectra is also sensitive to the composition of material, i.e. the nature of counter ion, degree of hydration of sample. In dehydrated sample, quadrupolar effects are so strong that the tetrahedral Al line disappears, reappearing on dehydration. No effect is observed for the octahedrally bound aluminum with changing degrees of hydration.

Table 2.9 NMR properties of selected nuclei

Isotope	Spin	Natural abundance (%)
^{1}H	1/2	99.98
^{23}Na	3/2	100
^{27}Al	5/2	100
^{29}Si	1/2	4.70
^{129}Xe	1/2	26.44
^{205}Tl	1/2	70.50

2.7.6 Temperature-programmed desorption of ammonia (NH_3-TPD) [29]

Temperature-programmed desorption of ammonia (NH_3-TPD) is the most widely used method to measure the acidic property of solid in mesoporous materials. On widely various solid-acidic catalysts, it was clarified that desorption was controlled by the equilibrium between the adsorbent and the adsorbed ammonia under usually utilized experimental conditions. There are many variations on the method but it typically involves saturation of the surface with ammonia under some set of adsorption conditions, followed by linear ramping of the temperature of the sample in a flowing inert gas stream. The amount of ammonia desorbing above some

characteristic temperature is taken as the acid-site concentration, and the peaks desorption temperature (T_M) have been used to calculate heats of adsorption. It is well- known that desorption temperature of the ammonia molecule can be related to the strength of acidity of the materials tested. The bond formed between the acid site and the ammonia is broken by an energy supply. Thus, the maximum temperature in the NH_3 desorption process is a qualitative indication of the strength of the acidic sites.

2.8 Cracking reaction

Cracking is the reaction to breaking up large molecules (lower value or useless feedstock) into smaller and more useful molecules. This is achieved by using high pressures and temperatures without a catalyst (thermal cracking or pyrolysis), or lower temperatures and pressures in the presence of a catalyst (catalytic cracking). There is not any single unique reaction happening in the cracker. A conventional chemical reaction of glycerol was studied with thermal only. The chosen catalysts are solid-acidic catalyst with high surface areas because it easy to separate and avoid corroding cracking reactors for increasing the activity. The major difference between thermal cracking and catalytic cracking is the initiator that the reaction through catalytic cracking occurred *via* ionic reaction, whereas the reaction through thermal cracking occurred *via* radical intermediate as shown in Figure 2.19. Carbocation has longer life and accordingly more selective than free radicals, therefore, the catalytic cracking product can be controlled more easily than those of thermal cracking.

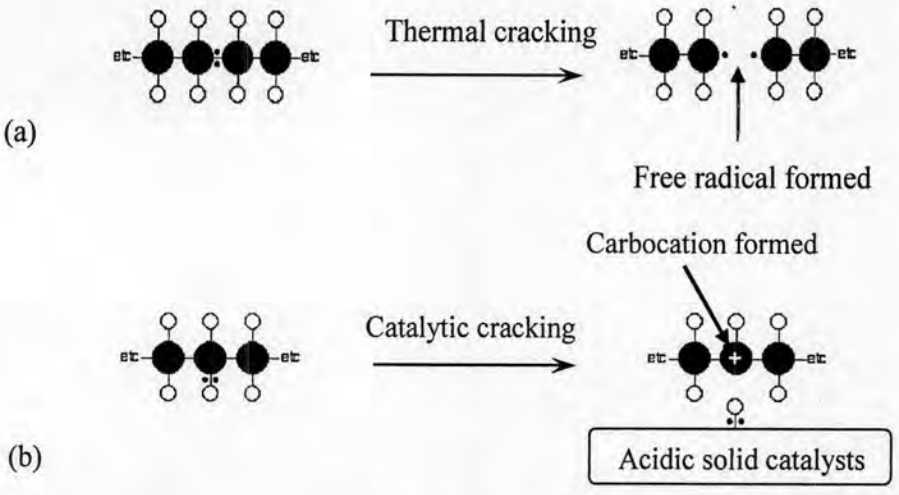

Figure 2.19 Model for cracking of hydrocarbon *via* (a) thermal cracking and (b) catalytic cracking.

2.8.1 Thermal cracking [46]

In thermal cracking, the high temperatures (~ 800°C) and pressures (~ 700kPa) are used in breaking the large molecules into smaller ones. The mechanism in thermal cracking began when the initiating radicals are formed by spontaneous bond rupture. The radical parts of the reaction mechanism are: initiation reaction, β-scissions, hydrogen transfer reaction, radical isomerization, radical additions, radical dehydratizations, radical substitutions, and radical termination reactions as concluding in Table 2.10.

Table 2.10 Reaction types to be considered in the free radical part of the reaction mechanism [10]

Reaction type	Example
1. Initiation reaction	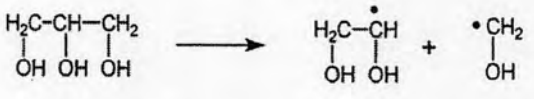
2. β-Scission	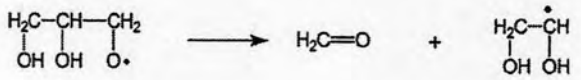
3. Hydrogen transfer	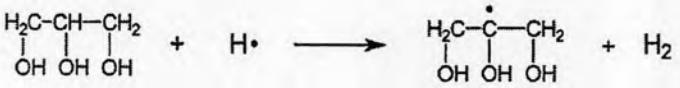
4. Radical isomerization	
5. Radical addition	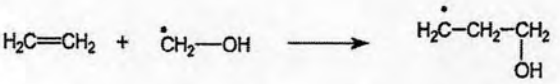
6. Radical dehydration	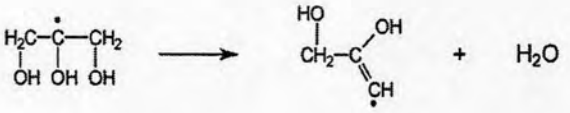
7. Radical substitution	
8. Radical termination reaction	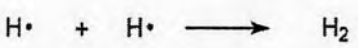

2.8.2 Catalytic cracking [47]

In catalytic cracking, mild conditions are used in breaking condition. The mechanism in catalytic cracking involves the ionic reaction. The reaction mechanism is totally based on assumptions as shown in Table 2.11.

Table 2.11 Reaction types to be considered in the ionic reaction part of the mechanism [10]

Reaction type	Example
1. Autoprotolysis	
2. Protonation	
3. Deprotonation by OH^--ion	
4. Dehydration	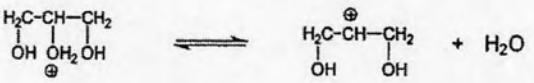
5. Keto-enol-tautomerization	
6. Acetalization	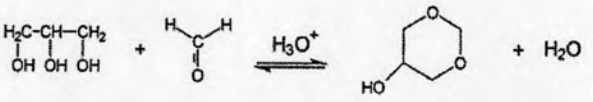
7. Aldol condensation	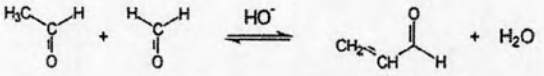

2.9 Application of product from the WBP cracking

After cracking reaction was complete, the gaseous product and the light liquid product were analyzed with GC. The major products of gas fraction were 1,3-butadiene and CO_2, whereas 2-cyclopenten-1-one was the main light liquid products.

2.9.1 1,3-Butadiene [48]

1,3-Butadiene seems to be the main gas product of waste from biodiesel production (WBP) cracking reaction. It is most utilized as synthetic rubber such as ABS, styrene-butadiene rubber *via* polymerization process by blend with styrene or acrylonitrile for ABS. In addition, other applications are apply for nylon production *via* the intermediate adiponitrile, create chloroprene (synthetic rubber materials), manufacture sulfolane (solvent) or produce cyclododecatriene.

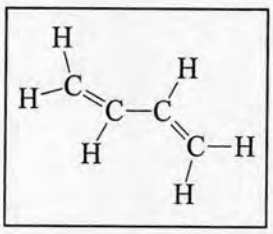

Figure 2.20 The structure of 1,3-butadiene.

Two processes are used to produce 1,3-butadiene from ethanol. In the single-step process developed by Sergei Lebedev, ethanol is converted to butadiene, hydrogen, and water at 400-450°C over any of a variety of metal oxide catalysts:

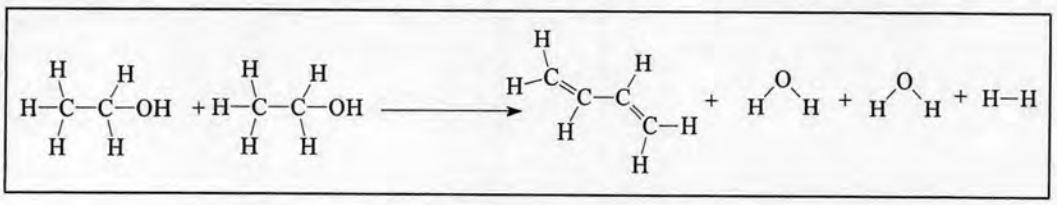

In the other, two-step process, developed by the Russian chemist Ivan Ostromislensky, ethanol is oxidized to acetaldehyde, which reacts with additional ethanol over a tantalum-promoted porous silica catalyst at 325-350°C to yield butadiene:

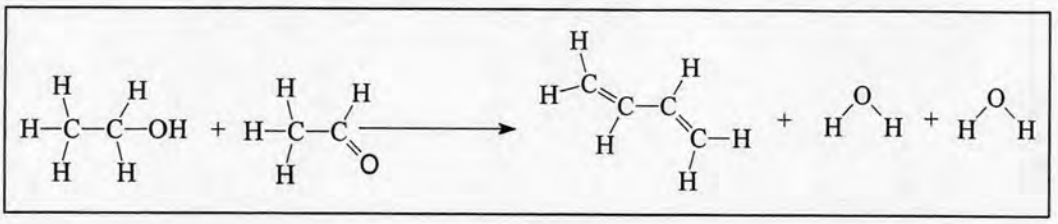

2.9.2 Carbon dioxide (CO_2) [49]

Carbon dioxide is one of the main gas products from WBP cracking reaction. It is used for photosynthesis and required for plant growth and development by plants. In addition, it is utilized in food and drink industry, in pneumatic systems, in fire extinguisher, in caffeine removal, in pharmaceutical and other chemical processing, in agriculture/biological applications, in polymers and plastics, in oil recovery, etc.

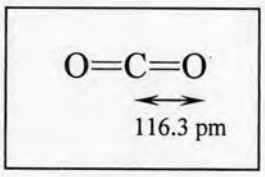

Figure 2.21 The structure of carbon dioxide.

For industrial production carbon dioxide is manufactured mainly from several processes such as from hydrogen plants, where methane is converted to CO_2, from combustion of wood and fossil fuels, from fermentation of sugar in the brewing of beer, whisky and other alcoholic beverages; from thermal decomposition of limestone ($CaCO_3$) or in the manufacture of lime (CaO), from sodium phosphate manufacture and directly from natural carbon dioxide springs, where it is produced by the action of acidified water on limestone or dolomite.

2.9.3 2-Cyclopenten-1-one [50]

2-Cyclopenten-1-one seems to be the major liquid product of WBP cracking. It is useful as an intermediate for perfumes (Jasmone and Jasmonate), medicines (Prostaglandin) and agricultural chemical.

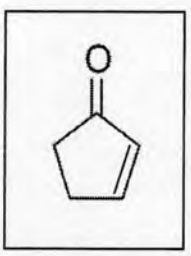

Figure 2.22 The structure of 2-cyclopenten-1-one.

In conventionally, 2-cyclopenten-1-one was synthesized by rearrangement of 4- cyclopentenones with an alkali such as KOH or Lewis acid such as BF_3 as catalyst or heated the reaction to 250-300°C in the case of non-catalysts condition. However, these methods gave low yield and produced large amounts of by-products. Thus, it is not satisfactory as an industrial method. 1,8-diazabicyclo-[5.4.0]undecene (DBU) or its organic salt as specific compounds catalyst was utilized for solving these problems by addition in the heating reaction. The rearrangement reaction of 4-cyclopentenones with the present of DBU performed high yield and easily in industry. Nowadays, 2-cyclopenten-1-one is able to synthesis *via* Nazarov cyclization or Pauson-Khand reaction [51-52].

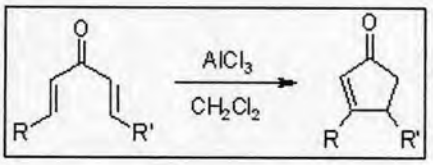

Nazarov cyclization

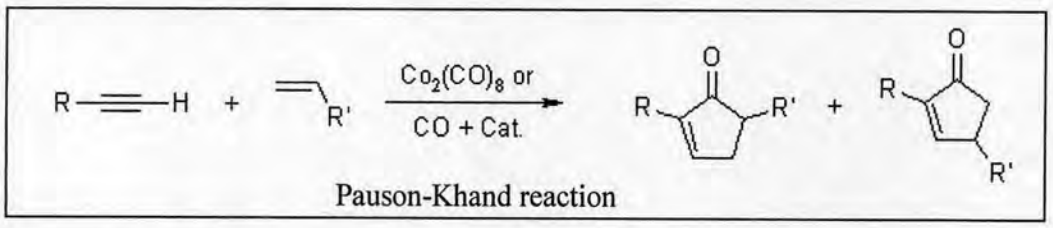

Pauson-Khand reaction

Figure 2.23 The reactions for synthesized 2-cyclopenten-1-one (a) Nazarov cyclization and (b) Pauson-Khand reaction.

Jasmone (Figure 2.24 (a)) is a natural organic compound extracted from the volatile portion of the oil from jasmine flowers. It is a colorless to pale yellow liquid. Jasmone can exist in two isomeric forms with differing geometry around the pentenyl double bond, cis- and trans- forms, with the cis- form predomination. Both forms have similar odors and chemical properties. It can act as either an attractant or a repellent for various insects. Commercially jasmine is used primarily in perfumes and cosmetics [53].

The jasmonates (JAs) are a group of plant hormones which help regulate plant growth and development. Jasmonates include jasmonic acid (Figure 2.24 (b)) and its esters, such as methyl jasmonate (MeJa) (Figure 2.24 (c)). Like the related prostaglandin hormones found in mammals, the jasmonates are

cyclopentanone derivatives which are derived biosynthetically from fatty acids. They are biosynthesized from linolenic acid by the octadecanoid pathway [54].

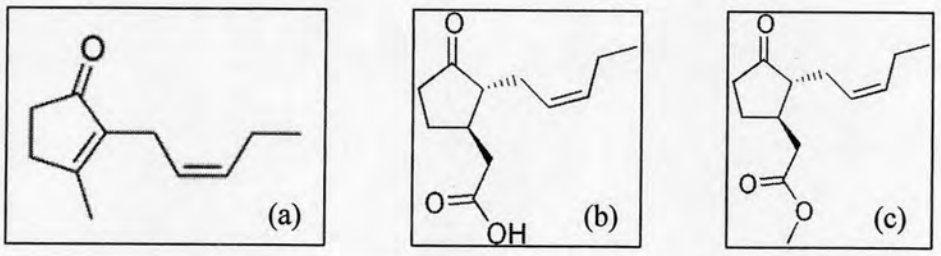

Figure 2.24 The structures of (a) jasmone, (b) jasmonic acid and (c) methyl jasmonate.

A prostaglandin is any member of a group of lipid compounds that are derived enzymatically from fatty acids and have important functions in the animal body. Every prostaglandin contains 20 carbon atoms, including a 5-carbon ring. They are mediators and have a variety of strong physiological effects; although they are technically hormones, they are rarely classified for example prostaglandin E_1, prostacyclin, etc. [55].

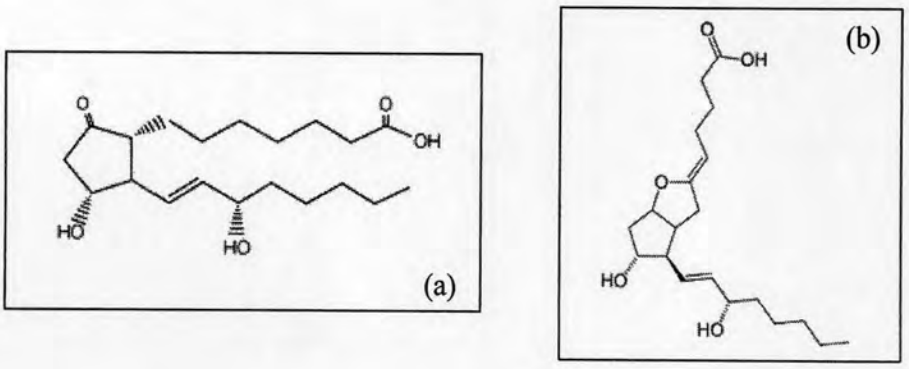

Figure 2.25 The structures of member of prostaglandin (a) prostaglandin E_1, (b) prostacyclin.